TEMPERATURE IN LASER-CREATED DEUTERIUM PLASMAS

J.L. BOBIN, F. DELOBEAU, G. DE GIOVANNI, C. FAUQUIGNON, F. FLOUX
Commissariat à l'Energie atomique, Villeneuve-Saint Georges,
France

ABSTRACT. The beam of a powerful neodymium glass laser is focused into a solid deuterium stick. The temperature of the created plasma is measured by Jahoda's X-ray absorption method. The electron temperature has been found to range up to 450 eV and exhibits a 2/3-power dependence on the power flux density.

These results are in agreement with a theoretical model involving a strong shock and a deflagration front propagating inwards the D_2 ice whereas the plasma expands in the vacuum towards the incoming beam.

Laser-created plasmas from solid-state targets with a fair amount of hydrogen isotope atoms have been investigated theoretically and experimentally [1 - 9]. Interest is focused either on plasma injection in fusion devices [4 - 6] or on direct generation of high-temperature plasmas [7 - 9]. In the latter case the target may be a solid surface (semi-infinite medium) or a roughly spherical small particle (total number of ions fixed).

The present paper deals with laser light interaction with massive solid-state Deuterium targets. The experiment is rather complicated. It involves a powerful neodymium glass laser, a sharp focussing and a cryogenic set-up. Only two diagnostic techniques are commonly used: streak recording of the plasma time history (fortunately deuterium ice is a transparent material) and electron temperature measurements by means of X-ray absorption.

Theoretical investigations were also made by using a simplified hydrodynamical model. Obviously, the model involves much more parameters than could actually be measured. However, the agreement between prediction and experimental results seems to be satisfactory.

1. EXPERIMENTAL SET-UP

The laser is a conventional C.G.E. Q-switched one. The oscillator stage uses a neodymium glass rod 300 mm long and 16 mm in diameter. A rotating prism provides the Q-switching and a triggering signal for diagnostic recording. The 30 ns, 3 J pulse is then amplified through a 5-rod-cascade up to 180 J. The laser has two cascades which may be used both or separately. Beam splitting occurs after the first amplifying rod. The pulse half-width depends on the oscillator geometry; it may vary from 30 to 80 ns owing to involuntary misalignment.

Shorter pulses were obtained by inserting a laser-beam triggered Pockels cell between the oscillator and the first amplifier. The overall exit aperture is 45 mm in diameter.

The beam is focused onto the target either by means of a specially devised aspherical single lens [10] or by an objective with three spherical lenses. They are mounted inside the same vacuum chamber as the target. Both of them are f/1.

The target is a solid deuterium stick. It is obtained by condensation of gaseous deuterium inside a copper extruder chilled by liquid helium. The cryogenic device is sketched in Fig. 1. The deuterium ice is a few millimetres long and has a 2 or 1 mm thick square cross-section.

The focal spot may be moved ± 2 mm with respect to the target surface.

To record the plasma time history we used an S.T.L. streak camera. The observation axis is perpendicular to the laser-beam axis.

The "plasma thermometer" is made of two thin plastic phosphors stuck on 56AVP03 photomultipliers. X-ray beams from the plasma are collimated and calibrated absorbers are inserted between source and detector. Under the assumption of a bremsstrahlung radiation spectrum, the ratio R of transmitted energies through two different absorbers is a given function of the source electron temperature [11]. We used Ni foils about 3 μm thick and extended Elton's calculations [12] to lower temperatures. Since the photomultipliers are not identical, the two ways of detection have to be carefully balanced: preliminary laser shots are made inserting the same material of equal thickness before the phosphors.

The X-ray recording set-up and a typical curve of R versus electron temperature are displayed in Fig. 2. Absorbers are selected to minimize the experimental error in the evaluation of temperature. Although the foils are carefully weighed before mounting, the accuracy of such measurements is no more than 20% for $T_e \sim 100$ eV and 10% for $T_e \sim 500$ eV.

Preliminary experimental results were disclosed in Refs [9] and [13]. Further experiments show the same qualitative behaviour which can be summarized as follows (Fig. 3):

The plasma appears first in the focal volume when a threshold value of about 10^{10} W/cm^2 is reached first.

Inside the ice the plasma growth towards the surface is perturbed by multiple breakdown phenomena (region I).

When the plasma has reached the free surface a strong expansion mainly directed towards the focusing lens occurs. At the same time a luminous front propagates rearwards into the target with a velocity close to 10^6 cm/s (region II).

Expansion in both directions is sometimes delayed by a few nanoseconds.

At last, when the plasma amount is very large, a cooling stage begins (region III) and develops as the laser is still delivering power to the plasma.

X-ray emission is contemporary with region II as shown in Fig. 4. The electron temperature turns out to be several hundreds of electron volts.

We are, therefore, mainly interested in the study of region II identified as the heating stage; a theoretical model was devised to cope with it.

2. THEORETICAL MODEL

To explain both expansion and inward propagation of the plasma the one-dimensional plane model involves a laser-supported deflagration which sustains a strong shock [14]. Both propagate inwards. The flow in a (X, t)-diagram and profiles are sketched in Fig. 5.

The origin of motion is at the ice-free surface. The laser radiation penetrates to R (see Fig. 5). The plasma generated and heated by light absorption above R is assumed to expand isothermally to the left. The boundary R between regions (E) and (S) of the flow is a discontinuity for the thermodynamic and kinematic variables, and also for the equation of state. (S) is a dense and a relatively cold medium. (E) is a high-temperature and moderate-density plasma.

The following further assumptions are made:

1) The flow is plane and one-dimensional. The shock is supposed to be established instantaneously at the origin of the process;

2) the discontinuity in the deflagration front implies negligibly small heat conduction. More exactly, heat conduction concerns only a very thin layer;

3) matter is described by a perfect-gas law in both media. (S) is a diatomic gas ($\beta = 1.4$), (E) is an elementary-particle gas ($\gamma = 1.67$);

4) (S) is loaded by a strong shock.

Radiation transfer and losses

Since the plasma in (E) is assumed to expand isothermally, the density distribution is related to the particle velocity u through

$$\rho = \rho_R \exp \frac{u - u_R}{c_T} \qquad (1)$$

where c_T is the so-called "thermal velocity" of sound:

$$c_T^2 = \frac{kT_R}{M}$$

where M is the molecular mass, T_R the plasma temperature and k the Boltzmann constant.

Using

$$u = \frac{x}{t} - c_T \qquad (2)$$

we find for a given time a density distribution exponential with respect to the abscissa; the scaling constant is $tc_T = L$.

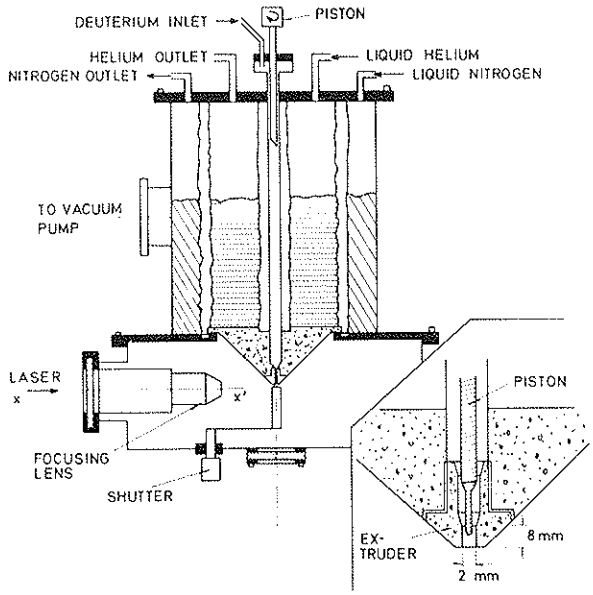

FIG. 1. Cryogenic device and interaction chamber. Gaseous deuterium is allowed to enter the cryostat and condensates within the copper extruder. Details are shown in the lower right corner. The exit hole dimensions may range from 0.5 to 2 millimeters. Thinner exits would require a different technology.

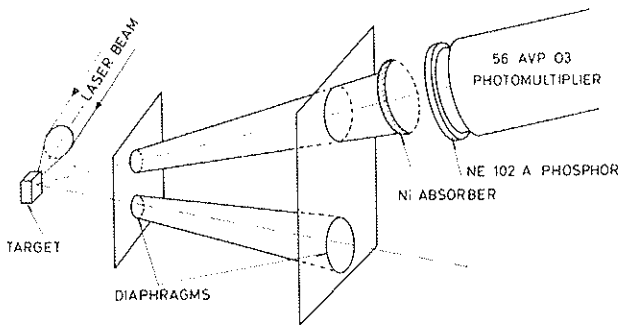

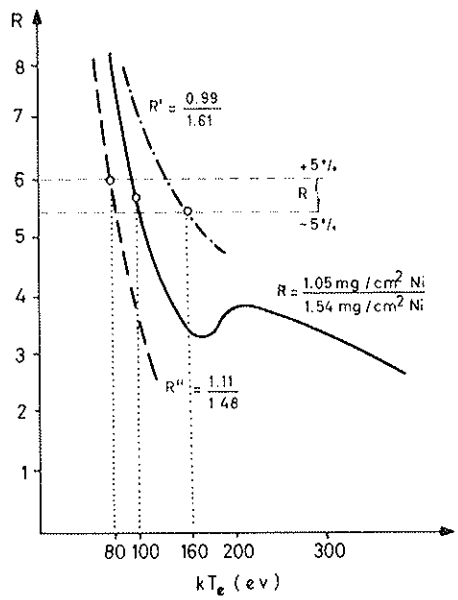

FIG. 2. X-ray apparatus and typical calibration curve.

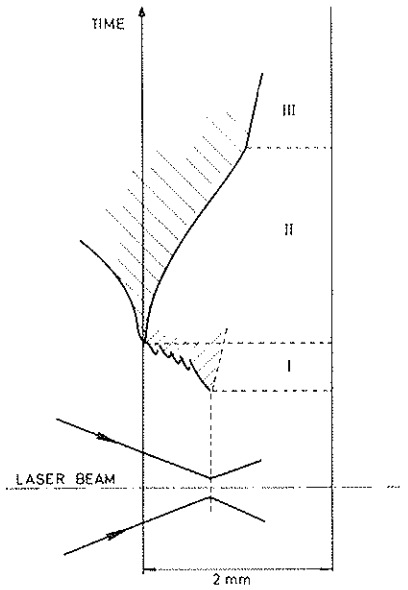

FIG.3. Plasma time history for a deuterium stick with a 2 mm square cross-section. Focusing is adjusted 7 millimeters inside the ice. Region II is the heating stage in the interaction process.

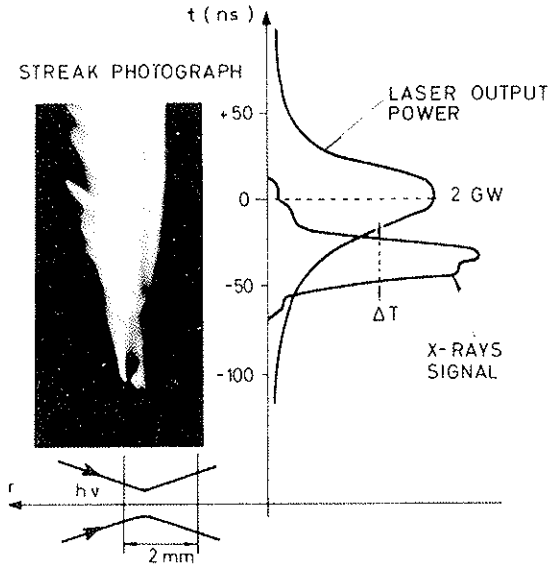

FIG.4. X-ray time history. X-ray signals are simultaneous with region II. In this experiment, the coupling between the laser pulse and hydrodynamics was rather poor and the electron temperature was therefore about 120 eV.

In such a profile laser light incident from the left will be absorbed provided that the density is less than the cut-off density:

$$\rho_c = \frac{\omega_0^2 m_e m_i}{4\pi Z e^2}$$

where ω_0 is the laser frequency, m_e the electron mass and m_i, Z the ion mass and charge, respectively. In the corresponding x_c, ρ_c plane light will be reflected and travel backwards.

Let Φ^+ and Φ^- be the light fluxes in the forward and backward directions. We may solve the transfer equation:

$$\frac{d\Phi}{dx} = -K\Phi$$

where according to Dawson and Oberman [15]

$$K_{\omega_0} = 4(2\pi)^3 \frac{Z^2 n_i n_e e^6 \log\Lambda}{3c\omega_0^2 (2\pi m_e kT)^{3/2}} \frac{1}{(1-\omega_p^2/\omega_0^2)^{\frac{1}{2}}} = \frac{a\rho^2}{\sqrt{1-b\rho}} \tag{3}$$

where ω_p is the plasma frequency for the density ρ.

The boundary conditions are

$$\Phi^+ = \Phi_0 \quad \text{for} \quad x = -\infty$$

$$\Phi^+ = \Phi^- \quad \text{for} \quad x = x_c$$

We find, thus,

$$\Phi_\infty^- = \Phi_0 \, e^{-\frac{8a}{3}\rho_c^2 L} \tag{4}$$

Thus provided $8a\rho_c^2 L/3 \gg 1$, i.e. the density gradient is not too steep, the incoming energy may be regarded as entirely absorbed.

Let us now consider the plasma radiation. We may use Eq. (3) and compare the radiation mean free path for a Planck distribution with the plasma dimensions. For temperatures of about 10^6 or 10^7°K, the plasma is transparent to its own radiation and the emission will be pure bremsstrahlung.

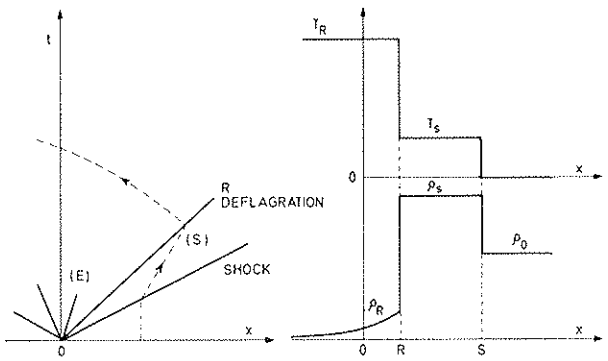

FIG.5. Scheme of the theoretical model. The flow is described on the (X, t) diagram (left) by a shock front followed by a deflagration R. The curves on the right are the density and temperature profiles for a given instant. On both graphs laser light comes from the left.

The emitted power is given by

$$P_\rho = 1.29 \times 10^{20} \rho^2 T^{\frac{1}{2}} \ \text{erg/cm}^3\,\text{s} \tag{5}$$

Substituting (1) and (2) into Eq. (5) and integrating over x from $-\infty$ to x_R we get

$$P = 4.16 \times 10^{20} \rho_R^2 T_R \tau \ \text{erg/s} \tag{6}$$

The volume dependence of the radiative losses appears through the duration τ of the flow. Al-

though expression (6) has been established for constant laser flux it indicates, in a more general way, the interest in short pulses. The numerical calculations were performed with a value of $\tau = 10^{-8}$ s.

Energy balance equation

At any given instant the total energy $\mathscr{E}_E$ is shared between the two parts (S) and (E):

1) the total energy transferred to (S) is given by

$$\mathscr{E}_S = M_S u_S^2$$

M_S being the shocked ice mass at time t, and u_S the particle velocity behind the shock front.

2) the total energy transferred to (E) can be written as

$$\mathscr{E}_E = \underset{\text{internal energy}}{\mathscr{E}_{Ei}} + \underset{\text{kinetic energy}}{\mathscr{E}_{Ek}} + \underset{\text{radiative losses}}{\mathscr{E}_{Er}}$$

Let M_R be the mass of deuterium having passed through (R) and u_R the particle velocity in (R). Then we have

$$\mathscr{E}_{Ei} = \frac{\gamma M_R c_T^2}{\gamma - 1}$$

$$\mathscr{E}_{Ek} = \int_{\alpha_R}^{\infty} \rho \frac{u^2}{2} dx = M_R \left[\frac{u_R^2}{2} + c_T^2 - u_R c_T \right]$$

$$\mathscr{E}_{Er} = \int P \, dt$$

with P given by expression (6).

The incoming laser flux is totally absorbed in (E) and transferred to the overall flow

$$\Phi_0 = \frac{d(\mathscr{E}_S + \mathscr{E}_E)}{dt} = \frac{d}{dt} \left[M_S u_S^2 + M_R \times \left(\frac{2\gamma - 1}{\gamma - 1} c_T^2 - c_T u_R + \frac{u_R^2}{2} \right) \right] \quad (7)$$

The number of variables in Eq. (7) may be reduced to 2 by:

1) taking into account the mass and momentum transfer equations through the shock and deflagration planes;

2) noting that D_2 (deflagration velocity) is close to u_S thanks to the large density jump through R and thus the small amount of matter flowing through this front.

u_S and T_R were chosen as independent variables that

$$\Phi_0 (u_S, T_R) = \frac{c_T}{4} \left[\frac{7\gamma - 5}{\gamma - 1} - \left(\frac{u_S}{c_T} \right)^2 \right] \frac{\beta + 1}{2} \rho_0 u_S^2 + P \quad (8)$$

We need one more equation involving u_S and T_R. Assuming thermal conduction (electron or radiative) to be negligible, the density at x_R depends only on the laser light frequency ω_0 and since radiation cannot propagate in a plasma denser than the cut-off value, one should have

$$\omega = \omega_p \quad \text{for } x_R$$

For deuterium and neodymium glass laser light the critical density is

$$\rho_c = \rho_R = 3.4 \times 10^{-3} \text{ g/cm}^3$$

Now the required equation is given by conservation laws through the deflagration front

$$u_S^2 (T_R) = \frac{4 \rho_R}{(\beta + 1) \rho_0} c_T^2 \quad (9)$$

Inserting expression (9) into Eq. (8) we obtain:

$$\Phi_0 (T_R) = \frac{c_T^3}{2} \rho_R \left[\frac{7\gamma - 5}{\gamma - 1} - \frac{4 \rho_R}{(\beta + 1) \rho_0} \right] + P \quad (10)$$

Other variables are easily calculated for a given laser flux and one may readily show that shock velocity and temperature T_R are proportional to $\Phi_0^{1/3}$ and $\Phi_0^{2/3}$ respectively, as far as the radiative losses are negligible compared to other energies appearing in the problem. A more detailed discussion of the model is given in Ref. [14].

Our results are to be compared with Caruso's who found $\Phi^{1/4}$ and $\Phi^{1/2}$ laws in a model [16] taking into account overall momentum conservation and using dimensional methods.

In contrast to previous investigations [17] we do not consider thermal radiation transport in the model. As will be shown in the next section we obtain satisfactory agreement with experimental results in the actual temperature range by ignoring thermal radiation.

3. INTERPRETATION OF EXPERIMENTAL RESULTS

Since earlier measurements various improvements have been made in the laser and diagnostic techniques. First, many shots were available showing a shorter laser-pulse rising time. Since at the beginning the pulse may be described mere exponentially: $P \sim P_0 \exp \alpha t$, α was found to be 1.6×10^8 s^{-1} instead of 10^8 s^{-1}. Thus electron temperatures up to 460 eV were observed. Optimal focusing is also different from previous experiments. The best coupling for light flux and hydrodynamics is found for a focal-spot position 1 mm inside the deuterium ice. It is worth noting that we used most generally laser amplification in a single cascade, and to operate a great number of shots the output energy was limited to 90 J, in practice.

Moreover, the plasma time history recording was improved by placing a Kodak blue filter before the S.T.L. photocathode and by using an electronic chronometer the accuracy of which is 0.1 ns.

Time matching is then obtained with an uncertainty of only 1 ns.

Smaller deuterium sticks 1 mm thick were also found to be useful; the inward propagating front of region II (Fig. 3) is allowed to reach the rear free surface as shown in Fig. 6. It is then easier to detect the propagating front and to measure its velocity D whose order of magnitude is a few 10^6 cm/s.

We are now able to compare the experimental values of the front velocity D, the laser light flux Φ and the electron temperature T_e with the theoretical predictions. As a rule, the measured electron temperature was naturally assigned to the region (E) of the model and refers to a plasma with comparatively low density.

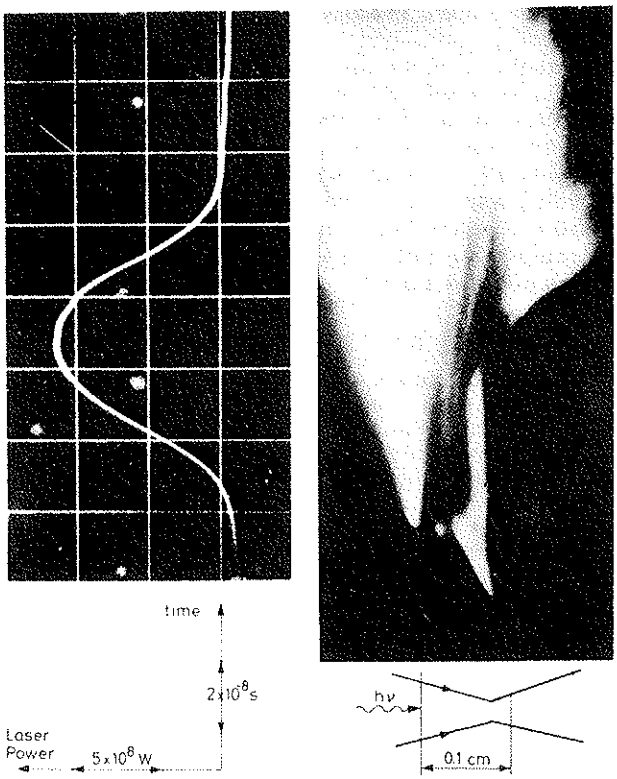

FIG. 6. Plasma time history in a 1 mm thick deuterium stick. The streak photograph and the laser pulse recording are placed relatively to the same time scale. Time runs upwards.

Since many streak pictures show lesser contrast than Fig. 6, the evaluation of D is often rather inaccurate. Calculating Φ by means of Eqs (9) and (10) would then yield rather doubtful results. Thus, we used an alternative method: the uncertainties in the time measurements are very small. Therefore, the position r of the propagating front and instantaneous laser power can be accurately related through time matching. Since we also have a fair knowledge of the focused beam geometry and flux distribution in vacuo, we can calculate at any time the flux which would impinge on the target if its refractive index were equal to 1. When plotted versus position the flux would follow the dashed curve in Fig. 7.

The corresponding maximum electron temperature calculated by means of formula (10) is found too high by a factor of about 2 which implies flux too large by a factor of about 5. This result is obtained with a focal spot 100 μm in diameter actually measured in vacuo. If a reasonable supplementary aberration due to the imperfect diopter vacuum-deuterium ice is taken into account, a focal spot of diameter 170 μm provides a fair agreement between measured electron temperature and evaluated flux: (see solid line in Fig. 7). The experimental values range from 2.2 to 3.8×10^{12} W/cm^2 whereas the calculated values corresponding to 270 eV to 400 eV electron temperature range from 2 to 4×10^{12} W/cm^2.

Experimental and theoretical front velocities are also in agreement within the above-stated (large) errors. It is not yet possible to determine which front (deflagration or shock) is actually recorded on the streak pictures. However, the latter seems to be favoured by comparing experiment and model. Anyway, since the velocities are very close to each other, so are R and S, and our flux evaluation should not be altered by identifying the observed front with any discontinuity.

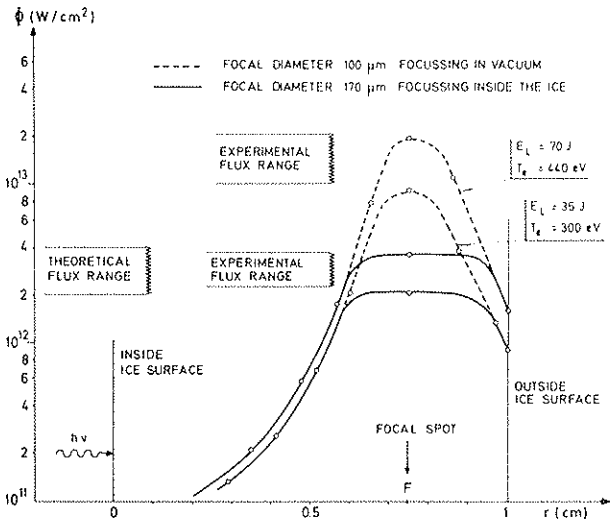

FIG. 7. Determination of the laser flux at the time and place of higher temperatures. The dashed curve is drawn for the focal region geometry recorded in vacuo. Taking into account a supplementary aberration yields the solid curve.

We notice also that if we substitute experimental T_e values into Eq. (4) the flux reflected backward is negligibly small.

For a given laser output energy and pulse shape, the measured electron temperature varies at random in a range not exceeding the experimental error. The final evaluation is obtained by averaging the data for about 20 shots. In Fig. 8 average electron temperatures are plotted versus maximum flux evaluated according to the above-described method. The few experimental points are in agreement with a $\Phi^{2/3}$ dependence for T_e as predicted by the theoretical model.

All the previous methods and results apply to laser pulses only slightly differing from the "standard" 30-ns-pulse. A tentative experiment was undertaken with shorter (nanosecond) pulses. These were obtained when inserting in the cascade a Pockels cell triggered by the oscillator standard laser pulse itself. The rising part may be described as two exponentials connected by a kink. During the second one (the steeper), the pulse increases by a factor up to 10^3 in 3 ns. Unfortunately, it was not possible to perform experiments with an output energy higher than about 15 J: a too large backwards flux is reflected towards the cascade and amplified until it reaches a fracture threshold for glass and partly destroys the laser.

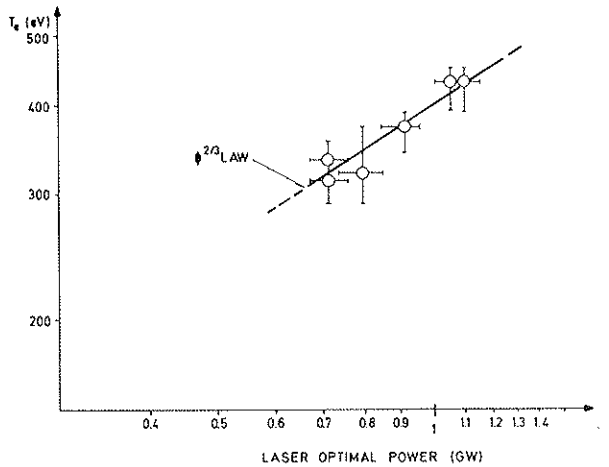

FIG.8. Plot of measured electron temperature versus the laser optimal power on logarithmic scales. The latter is derived from Fig.6 for a given laser shot. The laser flux considered in Eq.(10) turns out to be proportional to the optimal power.

However, it was possible to perform a few shots for 12 J of output energy. An average electron temperature of about 250 eV was obtained. We may infer from destructive shots that according to Eq.(4) the density gradient in region (E) is likely to be very steep in such experiments.

Another preliminary experiment was also made on the following grounds: in section II we deliberately ignored the influence of thermal radiation. It might not be true if a very high temperature (say 1 KeV) could be reached. Then it would be highly desirable to prevent energy losses due to thermal radiation diffusion through the colder medium. A material with higher Z would be suitable. A similar conclusion was also stated by Kidder [18]. To check such ideas a small percentage of krypton atoms was introduced into the deuterium ice. The shots were performed with a wider laser pulse: about 80 ns half-width and about 50 J output. In this case the average electron temperature was 450 eV.

4. CONCLUDING REMARKS

The experiments prove the existence of a high-temperature plasma when the beam of a powerful Q-switched neodymium glass laser is focused on solid deuterium. The simple theoretical model seems to be suitable to describe the actual interaction process. However, the diagnostics available were rather few. They have to be refined and confirmed by different measurements. In particular, we plan to determine the electron density profile throughout the various regions by holographic techniques [19].

According to the model, the high-temperature region is correlated with a rather low-density plasma:

$$\rho \leq \rho_R = 3.4 \times 10^{-3} \text{ g/cm}^3$$

Nevertheless, since the exponential decrement remains slow enough (this is to be checked experimentally) the obtained plasma with a density of about 10^{20} ions/cm^3 and a temperature of several hundreds eV looks promising. Then multi-kilovolt plasmas seem to be achievable with a suitable coupling between the laser parameters (brightness and pulse shape), and the focusing conditions onto the target.

REFERENCES

[1] BASOV, N.G., KROKIN, O.N., in quantum electronics (Proc. Int. Conf. Paris, 1963, 2 (1964) 1373.
[2] DAWSON, J.M., Phys. Fluids 7 (1964) 981.
[3] HAUGHT, A.F., POLK, D.H., Physics Fluids 9 (1966) 2047.
[4] SAUNDERS, P.A.H., AVIVI, P., MILLAR, W., Phys. Lett. 24 (1967) 290.
[5] HAUGHT, A.F., POLK, D.H., FADER, W.J., in Plasma Physics and Controlled Nuclear Fusion Research (Proc. Conf. Novosibirsk, 1968) 1, IAEA (Vienna, 1969) 925.
[6] BOURABBIER, C., CONSOLI, T., SLAMA, L., Phys. Lett. 23 (1966) 236.
[7] ASCOLI-BARTOLI, U., de MICHELIS, C., MAZZUCATO, F., in Plasma Physics and Controlled Nuclear Fusion Research, Proc. Conf. Culham, 1965, 2, IAEA (Vienna, 1966) 941.
[8] KIDDER, R.E., Nucl. Fusion 8 (1968) 3.
[9] COLIN, C., DURAND, Y., FLOUX, F., GUYOT, D., LANGER, P., VEYRIE, P., J. appl. Physics 39 (1968) 2991.
[10] CHAMPETIER, J.L., MARIOGE, J.P., de METZ, J., MILLET, F., TERNEAUD, A., C.r. hebd. Séanc. Acad. Sci., Paris 266 (1968) 838.
[11] JAHODA, F.C., LITTLE, E.M., QUINN, W.E., SAWYER, G.A., STRATTON, T.F., Phys. Rev. 119 (1960) 843.
[12] ELTON, C., ANDERSON, A., N.R.L. report 6541 (1967).
[13] BOBIN, J.L., FLOUX, F., LANGER, P., PIGNEROL, H., Phys. Lett. 28A (1968) 398.
[14] FAUQUIGNON, C., FLOUX, F., submitted to the Physics of Fluids.
[15] DAWSON, J.M., OBERMAN, C., Physics Fluids 5 (1962) 517.
[16] CARUSO, A., BERTOTTI, B., GUIPPONI, P., Nuovo Cim. 45B (1966) 176.
[17] VEYRIE, P., FLOUX, F., in A.I.A.A. Fluids and Plasma dynamics Conference, Los Angeles, (1968).
[18] KIDDER, R.E., A.I.A.A. Fluids and Plasma dynamics Conference, Los Angeles, (1968).
[19] BUGES, J.G., TERNEAUD, A., S.P.I.E. Seminar in-depth on Holography (San Francisco, 1968).

(Manuscript received 10 December 1968)